A 2D-Transmission Line Model for the EM Field Estimation Inside Enclosures with Apertures

I. Belokour
Visteon Corporation
P.O. Box 6010
Dearborn, MI 48120 USA
email:ibelokou@visteon.com

J. LoVetri
Department of Electrical Engineering,
The University of Manitoba,
Winnipeg, MB R3T 5V6, Canada
email:lovetri@ee.umanitoba.ca

Abstract

The development of efficient phenomenological models which give accurate estimates for the coupling of electromagnetic energy through apertures and into enclosures is important for the EMC design of almost all electronic subsystems. It has been previously shown that a simple analytical transmission line formulation gives good predictions of the dominant mode TE_{10} as well as higher-order modes TE_{m0} inside a rectangular enclosure with apertures. In this work the model is extended to include a two-dimensional set of transverse electric modes TE_{mn} in the transmission line (TL) model. The rectangular enclosure with aperture is represented as a intersection of two orthogonal transmission lines, one for each set of transverse electric modes. The model remains very simple and computationally efficient. The finite difference time-domain (FDTD) method is used to validate the results.

Keywords

phenomenological model, 2D-transmission line, electromagnetic energy, metal enclosure, aperture, transverse electric mode, finite-difference time-domain method

INTRODUCTION

Shielding is one of the most effective methods to protect against the disruptive effects of EMI. It prevents coupling of undesired radiated electromagnetic (EM) energy into equipment otherwise susceptible to it. Shielding effectiveness can be found by numerical methods or analytical approaches. An analytical approach to the shielding effectiveness estimation of a rectangular enclosure with aperture provides a cost-effective alternative to numerical methods, thus saving significant computing resources. It has been previously shown that for a simple system topology an analytical transmission line formulation gives good predictions of the shielding effectiveness of a rectangular enclosure with aperture [1], [2]. This formulation considers a single dominant mode propagating within the enclosure with aperture and is, therefore, limited to lower frequencies. This transmission-line model was expanded to include higher-order transverse electric (TE) and magnetic (TM) modes in [3]. However, these models are one dimensional and treat only a vertical polarization of the incident electromagnetic field. This limitation has motivated further research with the objective to extend the applicability of the model to the estimation of a transverse two-dimensional field pattern inside the enclosure with aperture which might be caused by the polarization of the incident EM field.

In this paper a new two-dimensional transmission-line model of an enclosure with aperture is presented which includes a two-dimensional set of transverse electric modes TE^{z}_{m0} and TE^{z}_{1n} propagating in the enclosure.

THEORETICAL INVESTIGATION

A rectangular enclosure with aperture with dimensions comparable to the wavelength range of disturbing electromagnetic energy acts mainly as a cavity resonator, supporting transverse electric (TE) and transverse magnetic (TM) waves. The distribution of the field inside some simple closed metal cavities can be understood as that existing in waveguide sections represented by transmission line structures with short-circuited ends which give rise to standing waves inside the enclosure. In a rectangular cavity with perfect conducting walls the distribution of the electromagnetic field can be modelled as a sum of TE_{mnp} and TM_{mnp} modes to any of the coordinate axis. These modes are the only possible solutions to Maxwell's equations that satisfy the boundary conditions of zero tangential electric fields on all walls [4].

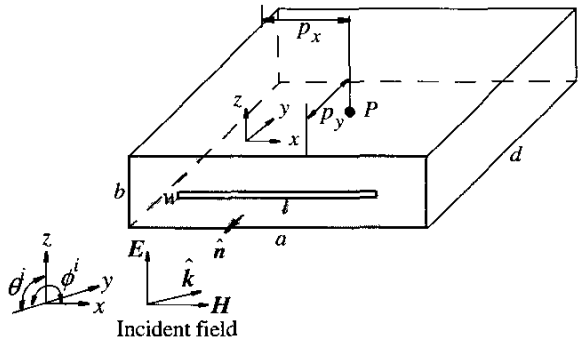

Figure 1. Geometry of the rectangular enclosure with a slot

A rectangular metal enclosure of length d, width a, and height b with a slot of length l and width w is shown in Figure 1. The coordinates of a test location P are p_x and p_y, respectively.

For a vertically polarized incident EM field, we consider TE^z_{m0} and TE^z_{1n} waveguide modes oriented in the z direction and propagating in the y and x directions respectively. For the dominant mode the condition that E_z be zero at $y = 0$ and $y = d$, as required by the perfect conductor walls, is satisfied if the dimension d is half the guide wavelength λ_g, that is

$$d = \frac{\lambda_g}{2} = \frac{\lambda}{2\sqrt{1-(\lambda/2a)^2}} , \tag{1}$$

The resonant frequency of the dominant cavity mode is given by

$$f_0 = \frac{\sqrt{a^2+d^2}}{2ad\sqrt{\mu\varepsilon}} , \tag{2}$$

where μ and ε is free-space permeability and permittivity, respectively.

For the m-th TE^z_{m0} and n-th TE^z_{1n} transverse electric modes of propagation, the enclosure is represented by a cavity formed by a section of shorted waveguide whose characteristic impedance, respectively, is

$$Z^y_{m0} = Z_0/\sqrt{1-(m\lambda/2a)^2} \tag{3}$$

$$Z^x_{1n} = Z_0/\sqrt{1-(n\lambda/(2d))^2} \tag{4}$$

and the propagation constant, respectively, is

$$k^y_{m0} = k_0\sqrt{1-(m\lambda/2a)^2}, \tag{5}$$

$$k^x_{1n} = k_0\sqrt{1-(n\lambda/(2d))^2} \tag{6}$$

where $Z_0 = \sqrt{\mu/\varepsilon}$ is the free-space impedance, $k_0 = 2\pi/\lambda$ is the free-space propagation constant, $m = 1, 2, 3, \ldots$ and $n = 1, 2, 3, \ldots$ is a wavenumber. When there is only one dominant mode in the enclosure then

$$Z_{m0} = jX_{m0} , \qquad (m \neq 1) \tag{7}$$

$$k_{m0} = -j\alpha_{m0} , \qquad (m \neq 1) \tag{8}$$

are imaginary. For $m = 1$, Z_{10}, is the real characteristic impedance of the dominant mode, and

$$k_{10} = \beta_1 - j\alpha_1 , \tag{9}$$

where $\beta_1 = 2\pi/\lambda_{g1}$ is the phase constant, λ_{g1} is the guide wavelength of the dominant mode and α_1 is the dominant-mode attenuation constant due to power loss in enclosure walls.

A rectangular aperture in the empty rectangular enclosure of Figure 1 is represented by the equivalent circuit of Robinson *et al.* [2]. The shunt impedance of the aperture of length l can be modelled as

$$Z_{ap} = \frac{1}{2}\frac{l}{a} jZ_{os}\tan\frac{k_0 l}{2}, \tag{10}$$

where Z_{os} is the characteristic impedance of the transmission line stub which models the aperture. A radiating source in the equivalent circuit of Figure 2 is represented by voltage V_0 and impedance Z_0. Combining Z_0, V_0 and Z_{ap} according to Thevenin's theorem gives an equivalent source voltage

$$V_s = (V_0 Z_{ap})/(Z_0 + Z_{ap}) \tag{11}$$

with a source impedance

$$Z_s = (Z_0 Z_{ap})/(Z_0 + Z_{ap}) . \tag{12}$$

Applying Bethe small-hole theory [5] to the slot in the enclosure front face shown in Figure 1, a transmitted field can be represented as the fields of a tangent magnetic dipole moment $\bar{p}_m$ and a normal electric dipole moment $\bar{p}_e$. Magnetic and electric dipole moments can be written as the product of the slot polarizability times appropriate incident field

$$\bar{p}_m = \alpha_m \bar{H}_t^{sc} \text{ and } \bar{p}_e = \varepsilon_0 \alpha_e \bar{E}_n^{sc} \tag{13}$$

where $\bar{H}_t^{sc}$ is the tangential magnetic field at the center of the short-circuited aperture and $\bar{E}_n^{sc}$ is the normal electric field at the center of the short-circuited aperture. The magnetic and electric polarizabilities, α_m and α_e, are given in [6] by

$$\alpha_e = \frac{\pi w^2 l}{16} \text{ and } \alpha_m = \frac{\pi l^3}{24\ln(4l/w) - 1} \tag{14}$$

For parallel polarization of the incident EM field, the short-circuited aperture fields are

$$H_t^{sc} = 2H_i \text{ and } E_n^{sc} = 2E_i \sin\theta^i . \quad (15)$$

For perpendicular polarization of the incident EM field, the short-circuited fields are

$$H_t^{sc} = 2H_i \cos\theta^i \text{ and } E_n^{sc} = 0 . \quad (16)$$

The transmitted field dependence on the incidence angle can be easily seen from eqs. (13)-(16). The variation in the incidence angle results in a $TE^z{}_{1n}$ component propagating in the x-direction.

THE ENCLOSURE EQUIVALENT CIRCUIT

The equivalent circuit of the rectangular enclosure with aperture is shown in Figure 2. It is represented by a intersection of two orthogonal sections of shorted waveguides of length d and a whose characteristic impedance and propagation constant are Z_{m0}^y, k_{m0}^y and Z_{1n}^x, k_{1n}^x, respectively. A radiating source in the enclosure equivalent circuit is represented by voltage V_0 and impedance Z_0. Point A corresponds to the location of the slot in the enclosure front face while point P corresponds to that of the test location. For typical rectangular enclosures the cutoff frequency of the dominant mode is of the order of hundreds of megahertz. This allows one to consider the ideal case and make the assumption that the wall losses are small compared to the energy which penetrates into the enclosure through the aperture. For the higher frequencies associated with the higher-order modes, the effect of ohmic loss in the cavity walls must be incorporated into the model [3]. The losses associated with a waveguide whose walls are not perfectly conducting can be modelled using the surface impedance concept as described in [4].

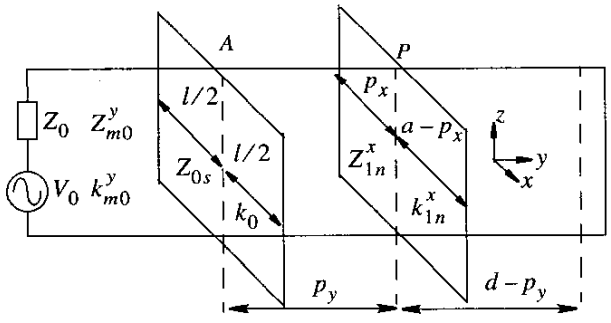

Figure 2. The equivalent circuit of a rectangular enclosure with aperture based on the transmission line model of shielding

Based on the transmission line theory given in [7] and the equivalent circuit shown in Figure 2, the impedance of the m-th mode Z_{rm0}^y viewed in the y-direction and n-th mode Z_{r1n}^x viewed in the x-direction at the test location P on the transmission line, respectively, is

$$Z_{rm0}^y = \frac{Z_l + jZ_{m0}^y \tan[k_{m0}^y(d-p_y)]}{1 + jZ_{m0}^{yn} \tan[k_{m0}^y(d-p_y)]}, \quad (17)$$

$$Z_{r1n}^x = \frac{Z_l + jZ_{1n}^x \tan[k_{1n}^x(a-p_x)]}{1 + jZ_{m0}^{xn} \tan[k_{1n}^x(a-p_x)]} \quad (18)$$

where Z_l is the termination impedance, $Z_{m0}^{yn} = Z_l/Z_{m0}^y$ and $Z_{n1n}^{xn} = Z_l/Z_{1n}^x$ is the normalized termination impedance for the m-th and n-th transverse electric mode, respectively.

The termination Z_l represents the surface impedance of the enclosure end wall given [4] as

$$Z_l = (1+j)\sqrt{\frac{\pi f \mu}{\sigma}} \quad (19)$$

where σ is the conductivity and μ is the permeability of the enclosure material, respectively. The termination Z_l includes the effect of ohmic losses in the enclosure walls into the estimation of an EM field intensity inside the enclosure. For perfect electric conductor walls of the enclosure with aperture the surface impedance of the end wall $Z_l = 0$, and this gives an effective impedance at test location P for the m-th mode Z_{rm0}^y and n-th mode Z_{r1n}^x, respectively, as

$$Z_{rm0}^y = jZ_{m0}^y \tan k_{m0}^y(d-p_y) \quad (20)$$

$$Z_{r1n}^x = jZ_{1n}^x \tan k_{1n}^x(a-p_x) \quad (21)$$

The source impedance Z_{lm0}^y and $Z^x{}_{l1n}$ of the m-th $TE^z{}_{m0}$ viewed in the negative to y-direction and n-th $TE^z{}_{1n}$ mode of propagation viewed in the negative to x-direction at test location P on the transmission line, respectively, is

$$Z_{lm0}^y = \frac{Z_s + jZ_{m0}^y \tan(k_{m0}^y p_y)}{1 + jZ_{m0}^{yn} \tan(k_{m0}^y p_y)}, \quad (22)$$

$$Z_{l1n}^x = \frac{Z_s + jZ_{1n}^x \tan(k_{1n}^x p_x)}{1 + jZ_{1n}^{xn} \tan(k_{1n}^x p_x)} \quad (23)$$

and the equivalent voltage V^y_{lm0} and V^x_{l1n} on the transmission line, respectively, is

$$V^y_{lm0} = \frac{V_s}{\cos(k^y_{m0}p_y) + jZ^y_{nm0}\sin(k^y_{m0}p_y)} \quad (24)$$

$$V^x_{l1n} = \frac{V_s}{\cos(k^x_{1n}p_x) + jZ^x_{n1n}\sin(k^x_{1n}p_x)} \quad (25)$$

The m-th TE^z_{m0} and n-th TE^z_{1n} mode voltage at test location P, respectively, is

$$V^y_{pm0} = V^y_{lm0}Z^y_{rm0}/(Z^y_{lm0} + Z^y_{rm0}) \quad (26)$$

$$V^x_{p1n} = V^x_{l1n}Z^x_{r1n}/(Z^x_{l1n} + Z^x_{r1n}) \quad (27)$$

and the total voltage of transverse electric TE^z_{m0} and TE^z_{1n} modes at the test location P on the transmission line, respectively, is now

$$V^y_{tpm0} = \sum_m V^y_{lm0}Z^y_{rm0}/(Z^y_{lm0} + Z^y_{rm0}) \quad (28)$$

$$V^x_{tp1n} = \sum_n V^x_{l1n}Z^x_{r1n}/(Z^x_{l1n} + Z^x_{r1n}) \quad (29)$$

One can see from (28) and (29) that the voltage at the test location P on the transmission line is proportional to the electric field produced by transverse electric modes.

The m-th and n-th mode current at the test location P, respectively, is

$$I^y_{pm0} = V^y_{lm0}/(Z^y_{lm0} + Z^y_{rm0}) \quad (30)$$

$$I^x_{p1n} = V^x_{l1n}/(Z^x_{l1n} + Z^x_{r1n}) \quad (31)$$

and the total current of transverse electric TE^z_{m0} and TE^z_{1n} modes at the test location P, respectively, is now

$$I^y_{tplm0} = \sum_m V^y_{lm0}/(Z^y_{lm0} + Z^y_{rm0}) \quad (32)$$

$$I^x_{tp1n} = \sum_n V^x_{l1n}/(Z^x_{l1n} + Z^x_{r1n}) \quad (33)$$

One can see from (32) and (33) that the current at the test location P on the transmission line is proportional to the magnetic field produced by transverse magnetic modes.

Thus, the expressions (28), (29) and (32), (33) can be used for the magnitude estimation of transverse electric modes propagating in the rectangular enclosure with aperture. The contributions of higher-order modes are computed by omitting the $m = 1$ or $n = 1$ term in equations (28), (29), or (32), (33).

NUMERICAL INVESTIGATION

The equivalent circuit shown in Figure 2 is used for computing the transverse electric TE^z_{m0} and TE^z_{1n} modes propagating in the rectangular enclosure with aperture. The enclosure and aperture dimensions are 0.3 m by 0.2 m by 0.12 m (length by width by height) and 0.025 m by 0.005 m (length by width), respectively. The transverse electric $TE^z_{10} - TE^z_{80}$ and $TE^z_{11} - TE^z_{18}$ modes are included in the transmission-line simulation. The ratio of the transverse electric $TE^z_{10} - TE^z_{80}$ and $TE^z_{11} - TE^z_{18}$ mode magnitude to the incident field intensity is computed at the test location P, respectively, as

$$S^y_{m0} = -20\log\frac{V^y_{tpm0}}{V_0} \quad (34)$$

$$S^x_{1n} = -20\log\frac{V^x_{tp1n}}{V_0} \quad (35)$$

The simulation results are shown in Figure 3 for the polarization angle of 45 degrees of the incident field. One can see that each of higher-order modes acts as a high-pass filter. The attenuation provided below cutoff, like that for a loss-free filter, is a reactive attenuation representing reflection but no dissipation. The resonant frequencies of the transverse electric $TE^z_{10} - TE^z_{80}$ and $TE^z_{11} - TE^z_{18}$ modes given in Table 1 are computed according to [7] as

$$(f_{res})^{TE}_{mnp} = \frac{1}{2\pi\sqrt{\mu\varepsilon}}\sqrt{\left(\frac{m\pi}{d}\right)^2 + \left(\frac{n\pi}{b}\right)^2 + \left(\frac{p\pi}{a}\right)^2} \quad (36)$$

where

$$m = 0, 1, 2, \ldots$$
$$n = 0, 1, 2, \ldots \qquad m = n \neq 0 \quad (37)$$
$$p = 1, 2, 3, \ldots$$

One can see in Figure 3 that the ratio of transverse electric mode magnitude to the incident field intensity is significantly increased at the respective resonant frequencies.

Table 1. Transverse electric $TE^z_{10} - TE^z_{80}$ and $TE^z_{11} - TE^z_{18}$ mode resonant frequencies

Mode order	1	2	3	4	5	6	7	8
TE^z_{m0}, MHz	901.4	1250	1677	2136	2610	3092	3579	4070
TE^z_{1n}, MHz	901.4	1581	2305	3041	3783	4528	5274	6021

This means that above the frequency of a dominant mode resonance, where the density of higher-order mode resonances increases, the enclosure compromised by apertures, slots or slits is not very effective as a shield. However, this relates only to a lossless enclosure with perfect electric conductor walls.

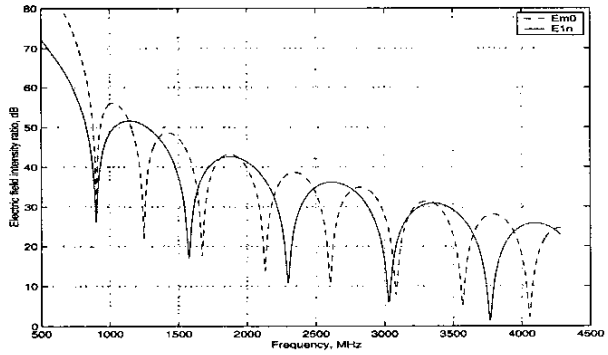

Figure 3. The electric field ratio at the test location *P* for $TE^z_{10} - TE^z_{80}$ and $TE^z_{11} - TE^z_{18}$ modes obtained by the transmission line simulation

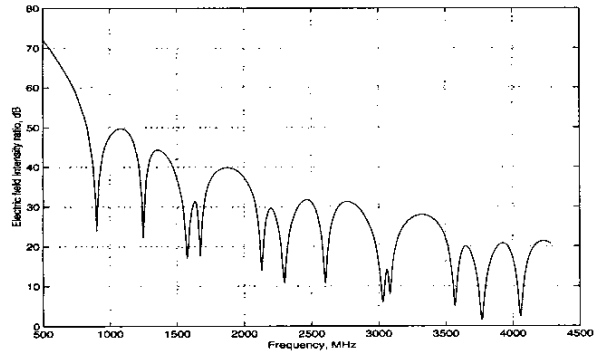

Figure 4. The electric field intensity ratio at the test location *P* obtained by the transmission-line simulation for $TE^z_{10} - TE^z_{80}$ and $TE^z_{11} - TE^z_{18}$ modes

The ratio of the electric field intensity at the test location P to the incident field intensity was obtained for the transverse electric $TE^z_{10} - TE^z_{80}$ and $TE^z_{11} - TE^z_{18}$ modes as

$$S = -20\log\frac{\sqrt{\sum_m (V^y_{tpm0})^2 + \sum_n (V^x_{tp1n})^2}}{V_0} \qquad (38)$$

The obtained ratio of the electric field intensity is shown in Figure 4. One can see the increase of the electric field intensity at the test location P with frequency.

The accuracy of the developed model was investigated by comparing the electric field predictions inside the rectangular enclosure with aperture obtained by transmission line simulations with that obtained by full-field simulations using the FDTD technique [8]. An FDTD code utilizing the scattering formulation has been developed at *The University of Western Ontario, Canada* [9]. The source of excitation is a plane uniform Gaussian pulse incident on the front face of the enclosure with aperture. The incident electric field has a spatial variation in y-direction given by a Gaussian pulse. The ratio of the transverse electric $TE^z_{10} - TE^z_{80}$ and $TE^z_{11} - TE^z_{18}$ mode magnitude to the incident field intensity at the test location P obtained using the FDTD technique is shown in Figure 5.

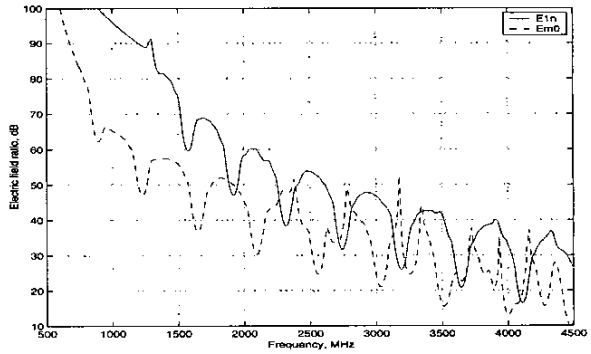

Figure 5. The electric-field ratio at the test location *P* for $TE^z_{10} - TE^z_{80}$ and $TE^z_{11} - TE^z_{18}$ modes obtained by the FDTD simulation

The ratio of the electric field intensity at the test location P to the incident field intensity obtained by the FDTD simulation is shown in Figure 6. One can see the increase of the electric field intensity at the test location P with frequency as well.

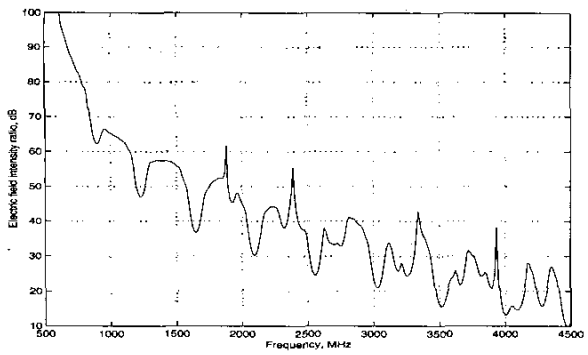

Figure 6. The electric field intensity ratio at the test location *P* obtained by the FDTD simulation for $TE^z_{10} - TE^z_{80}$ and $TE^z_{11} - TE^z_{18}$ modes

One can see from Figure 3 - Figure 6 that the electric field intensity at the test location *P* is very high at enclosure resonant frequencies. Losses are introduced in the enclosure to mimic the loading effect of electronics during numerical modelling. It is assumed that the losses are uniformly distributed throughout the enclosure. Distributed losses can be modelled in transmission lines by including a complex correction factor γ in the expressions for characteristic impedance and propagation constant [3].

CONCLUSIONS

An electromagnetic field inside a rectangular enclosure with aperture has been estimated based on a transmission-line approach. The 2D-transmission line model of a rectangular enclosure with aperture which includes transverse electric modes has been developed. The developed model is represented as a intersection of two orthogonal transmission lines, one for each TE^z_{m0} and TE^z_{1n} set of transverse electric modes, respectively. Distributed losses can be easily introduced into the modelled enclosure to mimic the loading effect of electronics. The model remains very simple and computationally efficient. A full-field FDTD technique is used for the validation of the developed model. It is evident from Figure 3 - Figure 6 that there is good agreement between the results obtained by the transmission line and FDTD simulations.

Estimation of the EM field coupled into a rectangular enclosure with aperture based on the 2D-transmission line approach offers a cost-effective alternative to the FDTD technique, saving significant computing resources. Solution time is the key advantage of the developed analytical method.

REFERENCES

[1] M.P. Robinson, J.D. Turner, D.W.P. Thomas, J.F. Disown, M.D. Ganley, A.C. Marvin, S.J. Porter, T.M. Benson and C. Christopoulos, Shielding Effectiveness of a Rectangular Enclosure with a Rectangular Aperture, *Electronic Letters,* vol. 32, no. 17, 1996, pp.1559-1560.

[2] M.P. Robinson, T.M. Benson, C. Christopoulos, J.F. Dawson, M.D. Ganley, A.C. Marvin, S.J. Porter, D.W.P. Thomas, Analytical Formulation for the Shielding Effectiveness of Enclosures with Apertures, *IEEE Trans. on Electromagnetic Compatibility,* vol. 40, no. 3, 1998, pp. 240-247.

[3] I. Belokour, J. LoVetri, and S. Kashyap, "A Higher-Order Mode Transmission Line Model of the Shielding Effectiveness of Enclosures with Apertures", 2001 *IEEE EMC International Symposium Proceedings,* Montreal, Quebec., pp. 702-707, 2001

[4] R. Collin, *Field Theory of Guided Waves*, McGraw-Hill Book Company, Inc., NY, 1960.

[5] H.A. Bethe, "Theory of Diffraction by Small Holes", *Physical Review,* vol. 66, no. 7 and 8, 1944, pp. 163-182.

[6] K.S.H. Lee, ed., *EMP Interaction: Principles, Techniques, and Reference Data*, Hemisphere Publishing Corp., Washington, DC, 1986.

[7] S.Ramo, J.R. Whinnery, T. Van Duzer, *Fields and Waves in Communication Electronics*, John Wiley & Sons, Inc.1994, 3rd edn.

[8] K.S. Kunz and R.J. Luebbers, *The Finite Difference Time Domain Method for Electromagnetics,* Bocca Raton, Fl, CRC, 1993.

[9] D. Mardare, R. Siushansian, and J. LoVetri, "3-D Dispersive EMFDTD", Version 1.3, The University of Western Ontario, Department of Electrical Engineering, Dec. 1995.